THREE DIMENSIONAL ANALYSIS OF RF ELECTROMAGNETIC FIELD BY THE FINITE ELEMENT METHOD

M. Hara, T. Wada, K. Mitomori
Cyclotron Lab., RIKEN Wako, Saitama 351-01 Japan
and F. Kikuchi
College of Arts and Sciences, The University of Tokyo

ABSTRACT

It is necessary to get eigensolutions of Maxwell's equations in order to design resonators for accelerators. The numerical computation of the solution, however, is very difficult especially in the arbitrary three-dimensional case. We have developed special finite element models with "exotic" nodal configurations for two and three dimensional elements. In these models, tangential component of electric field at each side of each element is taken as unknown variable and is constant on the side and continuous along the interelement boundaries. In this paper some mixed finite element models are presented with numerical results for two and three dimensional problems. Satisfactory results are obtained for simple problems.

1. INTRODUCTION

In the design of accelerators, resonator design is one of the most important part and it is necessary to calculate electromagnetic fields in cavities. In the design of cyclotron resonators, we usually use transmission line approximation which is basically one dimensional approximation and is inappropriate to get field distribution along dee gap. With the progress of computers, many numerical calculation codes have been developed to get rf characteristics of resonators. Most of these treat resonators of constant cross section or axi symmetric modes[1]. Recently Weiland has developed a three dimensional calculation code which is based on the finite difference method and uses only rectangular parallelepiped control volumes[2]. We have developed a true three dimensional calculation code which is based on the finite element method. In this model, we can use a rectangular parallelepiped element but also a trigonal prism element and a tetrahedral element. Then it is easier to apply to resonators of arbitrary shape and also to impose boundary conditions. In this paper we present the model and some calculation examples.

2. BASIC EQUATIONS

We deal with a time-harmonic electric field in vacuum of bounded region surrounded by a perfect conductor. It is described by Maxwell's equations which are reduced to

$$\mathrm{div}\ \mathbf{E} = 0, \qquad (1)$$
$$\mathrm{rot}\ \mathrm{rot}\ \mathbf{E} = \lambda \mathbf{E}, \qquad (2)$$

where $\lambda = \omega^2/c^2$.

Boundary condition is

$$\mathbf{n}\times\mathbf{E} = 0 \quad \text{on the surface}, \qquad (3)$$

where $\mathbf{n}$ is a unit vector normal to the surface.

In eq.(2),

for $\lambda \neq 0$ $\mathrm{div}\ \mathbf{E} = 1/\lambda\ \mathrm{div}(\ \mathrm{rot}\ \mathrm{rot}\ \mathbf{E}\ ) = 0$,

$\lambda = 0$ $\mathrm{rot}\ \mathbf{E} = 0$ but not $\mathrm{div}\ \mathbf{E} = 0$.

We must treat an eigenvalue problem for a real vector-valued function. A difficulty of this problem is in dealing with divergence-free condition (1).

3. NEW TYPE OF FINITE ELEMENT MODELS

We have already tested a penalty method[3]. The method was successful for very simple shape resonators, but not fully successful for complex shape. We propose here new types of finite element models which satisfies divergence free condition (1). These models have quite different node configurations from usual finite element ones because unknown variables are taken not on nodal points but on the sides of the element. We call this models as exotic models. These types of finite element models are not so new[4], and it can be seen as the extension of the Weiland's model[2].

Detailed formulation of this model is presented in ref.5 and here we only summarize the results. In that paper weak formulations for Maxwell's equations are presented which are based on the mixed and penalty methods. Mixed formulation is based on the Lagrange multiplier.

Characteristics of this model are as follows;

(1) Tangential components of the electric field on the sides of the element are adopted as unknown variables, which are constant on the sides.

(2) Divergence-free condition is fully satisfied in each element.

(3) Electric field is not strictly continuous, but only tangential component is continuous along the interelement boundaries.

(4) The handling of boundary condition is easy.

(5) Only five types of elements are in practical use.

In Fig. 1, five types of mixed finite element models with exotic nodal configurations are shown. In these elements, triangular element for two dimensional and axisymmetric case and tetrahedral element for three dimensional case are important for practical use.

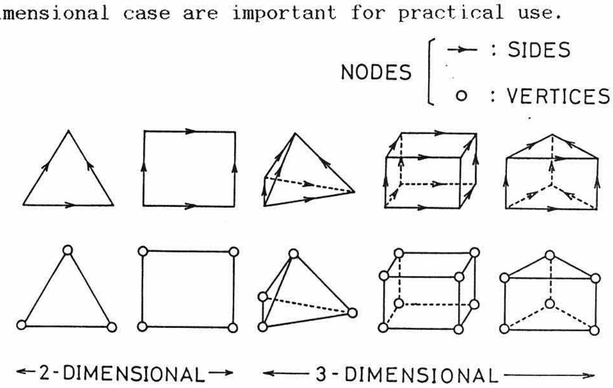

Fig. 1. Types of exotic element models.
Only these five types can be used for our new types of finite element models.
Upper and lower rows show the sides and nodes of the elements, respectively.

1. Triangular element

In finite element model of two dimensional case, we take the following approximation of **E** in an element:
(1) linear polynomial approximation.
(2) rot **E** = constant.
(3) div **E** = 0.
(4) Tangential component is constant on each side of the element.

Electric field **E** = (E_x, E_y), in this element, is written as

$$E_x = \alpha_1 + \alpha_2 y,$$
$$E_y = \alpha_3 - \alpha_2 x.$$

In these eqns., the coefficient of y in E_x and that of x in E_y have the same absolute value and opposite signs which comes from above condition (4).

Then $$\text{rot } E = \frac{\partial E_y}{\partial x} - \frac{\partial E_x}{\partial y} = -2\alpha_2,$$

and $$\text{div } E = \frac{\partial E_x}{\partial x} + \frac{\partial E_y}{\partial y} = 0.$$

In this element model, shape functions are given as follows:

$$E_x = \sum_{i=1}^{3} \frac{-l_i (y-y_i)}{2A} E_{s,i+3} S_i,$$

$$E_y = \sum_{i=1}^{3} \frac{l_i (x-x_i)}{2A} E_{s,i+3} S_i,$$

where s indicates side of i+3 in Fig. 2, and Si indicates the sign of i side length.

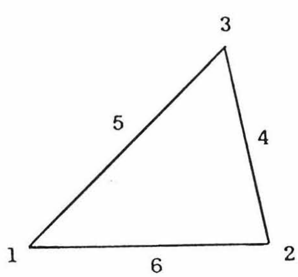

Fig. 2. Triangular element
Figures 1 to 3 indicate nodal points and 4 to 6 indicate sides. Tangential component of electric field on each side is constant on it and continuous but normal component is not continuous at the interface of elements.

From this expressions, element stiffness matrix M_s and element mass matrix M_m are

$$M_s = 1/A \ [\ l_i l_j S_i S_j\ ] \ ,$$

$$M_m = 1/4A^2 [S_i S_j l_i l_j \iint \{(x-x_i)(x-x_j) + (y-y_i)(y-y_j)\}\, dxdy$$
$$= 1/A[S_i S_j l_i l_j \{x_i^* x_j^* + y_i^* y_j^*$$
$$-1/6(x_1^* x_2^* + x_2^* x_3^* + x_3^* x_1^*$$
$$+ y_1^* y_2^* + y_2^* y_3^* + y_3^* y_1^*)\}\ ],$$

where A is the area of the element, l_i is the length of side of i+3, S_i is the sign of the side length, and $x_1^* = x_1 - x_M$ with x_M being the center of gravity.

2. Tetrahedral Element

Regions of arbitrary three dimensional shapes can be divided into tetrahedral elements with quite good approximation. In the same manner as two dimensional triangular element, the following conditions are required to this finite element model.
(1) linear polynomial approximation.
(2) rot **E** = constant.
(3) div **E** = 0.
(4) Tangential components are constant on each side of the element.

Electric field **E** = (E_x, E_y, E_z), in this element is written as

$$E_x = \alpha_1 + \alpha_2 y + \alpha_3 z\ ,$$
$$E_y = \alpha_4 - \alpha_2 x + \alpha_5 z\ ,$$
$$E_z = \alpha_6 - \alpha_3 x - \alpha_5 y\ .$$

Then $$(\text{rot } E)_x = \frac{\partial E_z}{\partial y} - \frac{\partial E_y}{\partial z} = -2\alpha_5\ ,$$

$$(\text{rot } E)_y = \frac{\partial E_x}{\partial z} - \frac{\partial E_z}{\partial x} = 2\alpha_3\ ,$$

$$(\text{rot } E)_z = \frac{\partial E_y}{\partial x} - \frac{\partial E_x}{\partial y} = -2\alpha_2\ ,$$

$$\text{div } E = \frac{\partial E_x}{\partial x} + \frac{\partial E_y}{\partial y} + \frac{\partial E_z}{\partial z} = 0\ .$$

Shape functions in this model are written as

$$E_x = 1/(6V)\sum_{i=1}^{6} l_i [(z_k(i) - z_m(i))y + (y_m(i) - y_k(i))z + (y_k(i)z_m(i) - y_m(i)z_k(i)] E_i S_i\ ,$$

$$E_y = 1/(6V)\sum_{i=1}^{6} l_i [(x_k(i) - x_m(i))z + (z_m(i) - z_k(i))x + (z_k(i)z_m(i) - z_m(i)x_k(i)] E_i S_i\ ,$$

$$E_z = 1/(6V)\sum_{i=1}^{6} l_i [(y_k(i) - y_m(i))x + (x_m(i) - x_k(i))y + (x_k(i)y_m(i) - x_m(i)y_k(i)] E_i S_i\ ,$$

where V is the volume, l_i is the side length of i side, E_i is the i side component of electric field and S_i is the sign of i side length. As shown in Fig. 3, i side indicates the circled i+4 side. Summation i indicates the i+4 side and m and k in that case are shown in Tab. 1.

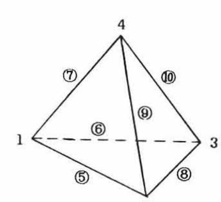

Table 1

i		k	m
1	5	3	4
2	6	4	2
3	7	2	3
4	8	1	4
5	9	3	1
6	10	1	2

Fig. 3. Tetrahedral Element
Nodal points are indicated with 1 to 4. Sides are indicated with 5 to 10 in circle. Tangential components on each side are constant and electric field at an arbitrary point in the element is expressed with the linear contribution of the tangential components of all sides.

The element stiffness and mass matrices for tetrahedral case are also given through the same procedure as the case of two dimensional, but the explicit expression is very complicate to write down.

4. ASSEMBLAGE AND BOUNDARY CONDITIONS

From the above procedure, element matrices are given. Then according to the usual finite element procedure, all the element matrices are assembled to total mass and stiffness matrices of the total matrix equation.

Boundary conditions are imposed to the assembled matrices. For a metal surface, tangential components of electric field are zero. So the corresponding row and column are eliminated. For a mirror symmetric plane, no special constraint conditions need be imposed since this case may be treated as natural boundary conditions.

In this way, we can get the matrix equation and we must solve the generalized eigenvalue equation. These total matrices have many zero components and are usually very sparse. So usually some techniques are used to save computer memory. In this time we used skyline scheme for the Gauss elemination method[6].

5. NUMERICAL RESULTS

We made some calculations for several simple problems to check the validity of our approach.

1. Two dimensional problem

We calculated the field in a rectangular domain with a notch of depth a. Figure 4(a) shows two types of meshes. We calculated the lowest eigenvalue using triangular element. Using symmetric properties of the fields, only an upper half area is divided and calculated. Notch dependence(a) of the lowest eigenvalue is shown in Fig. 4(b) for 10×10B meshes. In this figure solid line indicates the results obtained with the conventional method[1]. The calculated eigenvalues show good agreement with conventional method and the eigenvalue dependence on a is consistent with the perturbation theory. Figure 4(c) shows the field

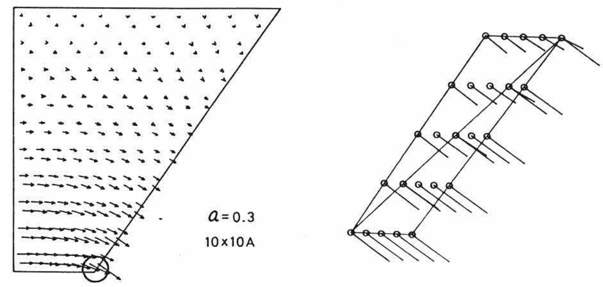

(c) (d)

Fig. 4(c). Electric fields calculated at the center of mass of each triangular element.
Fig. 4(d) Electric fields in two triangular elements at the edge indicated by the circle in Fig.4(c).
In these figures, eigenvalue and eigenvectors are calculated on the sides of elements, and from these values electric fields at arbitrary points are calculated.

distribution calculated at the center of mass of each triangular element. In Fig. 4(d), the field in two triangular elements at the edge are shown. Bars indicates the magnitude and direction of electric fields. Electric fields at element interfaces have different values which depends on the element. In this model, only tangential components are continuous. By the same reason, the exact electric fields should have no normal component on the symmetry plane, but the calculated ones have small amount as it is. This kind of errors are inherent in this method.

2. Three dimensional problem

First we calculated a simple parallelepiped cavity. Obtained results were quite reasonable. Figure 5 shows the convergence of eigenvalue for 3×4×5 size parallelepiped cavity. Division of more than 4×4×4 gives sufficient convergence for the eigenvalue in this case.

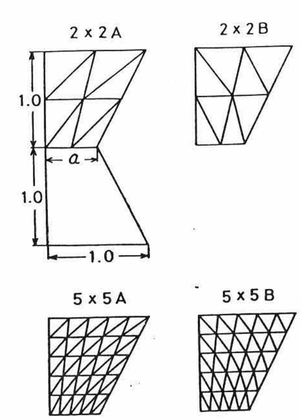

(a)

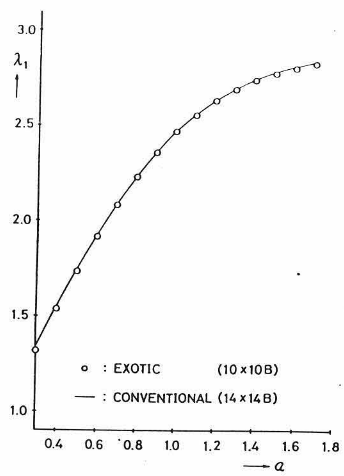

(b)

Fig. 4(a). two dimensional mesh.
Fig. 4(b). calculated eigenvalue.
Notch depth dependence on eigenvalue is shown. The results show good agreement with the calculation with conventional finite element model.

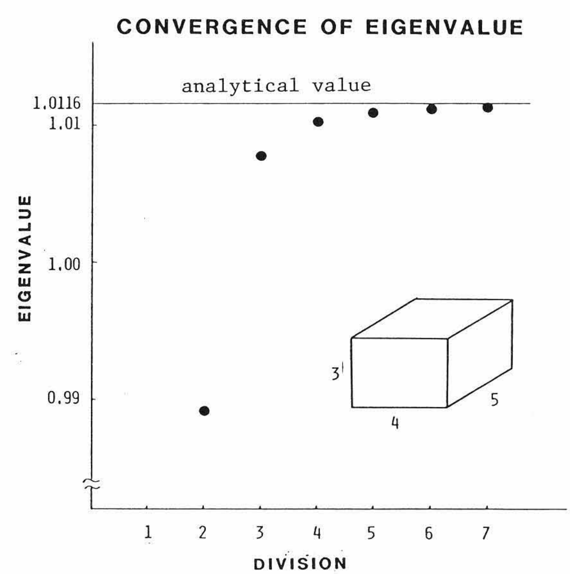

Fig. 5. Convergence of eigenvalue with division N.
For such a simple parallelpiped cavity, convergence is very fast.

Secondly, we calculated a deformed parallelepiped cavity. Figure 6 shows the lowest eigenvalues with deformation x. This variation of the eigenvalue consists with the perturbation theory. That is, when the volume where electric field is strong is reduced, eigenvalue should be reduced. Calculated electric field is shown in Fig. 7 by vector plots.

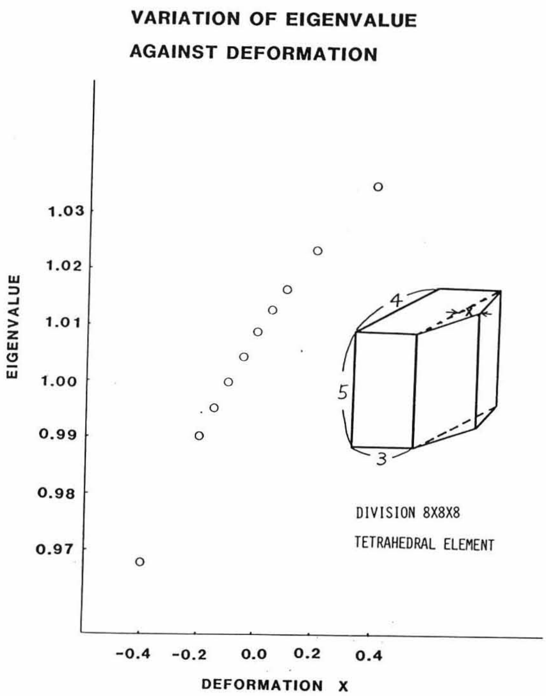

Fig. 6. Variation of eigenvalue against deformation

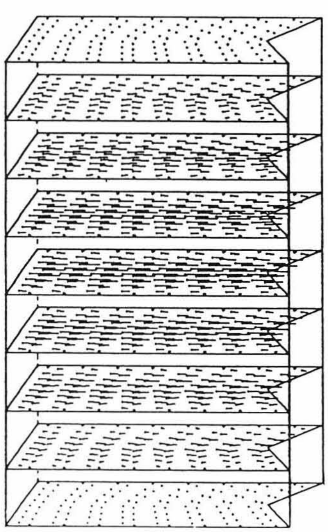

Fig. 7. Electric field distribution for deformed parallelpiped cavity. Electric fields which are calculated at the center of mass of each triangle on z-sliced planes are indicated.

It is well known that in three dimensional calculations large size of computer memory is required. We have estimated the required size. Figure 8 shows the required memory size vs division number N. This figure shows that the required memory has N^5 dependence. It is because the skyline scheme is adopted for the solver. When the division is N, the order of matrix is nearly proportional to N^3. In the skyline scheme, bandwidth is nearly proportional to N^2. So required memory size is approximately proportional to N^5. According to our mesh generator program, maximum nonzero components of one column or row, is expected to be 19 considering the symmetry of the matrix. So the minimum size of memory to store the matrix is about $19 \times N^3$, which line is also indicated in this figure. At present we are developing a computer code based on some iteration methods which can take advantage of this storage property.

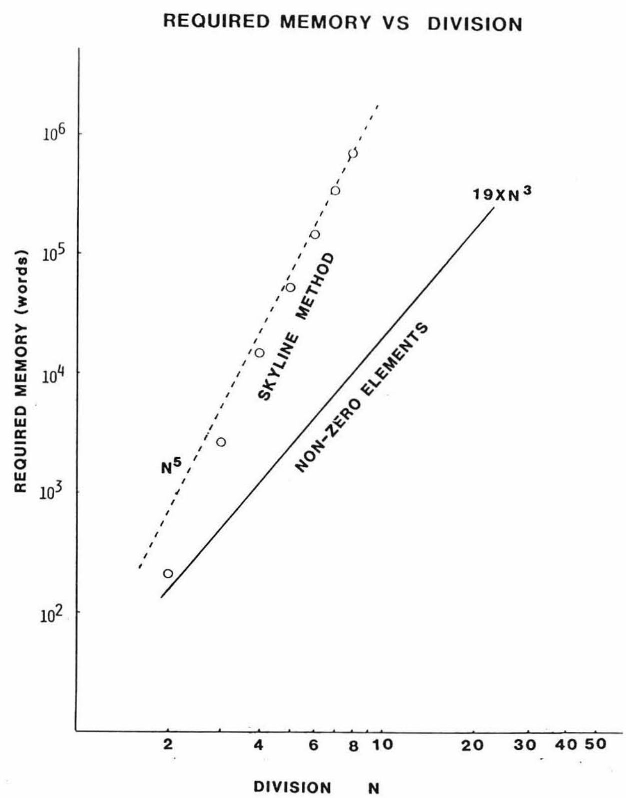

Fig. 8. Required memory vs division N.

REFERENCES

(1)M.Hara, T.Wada, A.Toyama and F.Kikuchi, Sci. Papers IPCR 75 (1981), 143.

(2)T.Weiland, Particle Accelerators 15 (1984), 245.

(3)M.Hara, T.Wada, T.Fukasawa and F.Kikuchi, IEEE Trans. Mag. 19 (1983), 2417.

(4)J.C.Nederic, Numer. Math. 35 (1980), 315.

(5)F.Kikuchi, "A finite element method for 3-D analysis of cavity resonators", in preparation.

(6)K.J.Bathe and E.L.Wilson, Numerical Methods in Finite Element Analysis, (1976), Prentice-Hall.